SciencePG
Science Publishing Group

Using Modified Activated Carbon to Remove Methylene Blue and Rhodamine B from Wastewater

N'guessan Louis Berenger Kouassi[1, *], Abollé Abollé[2], Adjoumani Rodrigue Kouakou[2], Victor Gogbe[2], Albert Trokourey[3]

[1]Department of Mathematics, Physics and Chemistry, University of Peleforo Gon Coulibaly, Korhogo, Ivory Coast

[2]Laboratory of Thermodynamic and Physical Chemistry of the Environment, University of Nangui Abrogoua, Abidjan, Ivory Coast

[3]Laboratory of Constitution and Reaction of Matter, University of Felix Houphouet Boigny, Abidjan, Ivory Coast

Email address:

kberenger2015@gmail.com (N'guessan Louis Berenger Kouassi)

[*]Corresponding author

Abstract: Water contamination by dyes is a worldwide problem. There is, however, limited information on the adsorption of rhodamine B (RhB) and methylene blue (MB) by activated carbon modified by ethylenediaminetetraacetic acid (EDTA). This study aimed to remove MB and RhB from industrial effluent by palm kernel shell modified activated carbon. The specific surface area (S_L), and the zero charge pH (pHpzc) for unmodified activated carbon (AC) and modified activated carbon (AC-EDTA) were determined. The AC and AC-EDTA were also characterized by Raman spectroscopy and Fourier transform infrared spectroscopy (FTIR). In the synthetic solutions and real effluents, the batch experiments were used to evaluate the MB and RhB adsorption capabilities by AC and AC-EDTA. The pHpzc values were 5.4 and 4.1 for AC, and AC-EDTA, respectively. The specific surface areas were found to be 756 m^2/g and 538 m^2/g for AC and AC-EDTA, respectively. The FTIR results indicated that C-N, N-H, and C=O functional groups were introduced onto the surface of activated carbon after in situ EDTA modification. The degree of graphitization (R) values were 0.63 and 0.78 for AC and AC-EDTA, respectively. The study indicated that the second-order and Langmuir models best fitted MB and RhB adsorption. In the synthetic solution, methylene blue maximum adsorption capacities (Qmax) were 5.5 mg/g and 7.40 mg/g for AC, and AC-EDTA, respectively. Rhodamine B's maximum adsorption capacities were 3.82 mg/g, and 7.11 mg/g for AC, and AC-EDTA, respectively. In the industrial effluent, the methylene blue removals percentages by AC and AC-EDTA were 59.83% and 79.98%, respectively. Those of rhodamine B were 12.9% and 58.71%, respectively for AC and AC-EDTA. Thus, the MB and RhB adsorption capacities were enhanced by AC-EDTA.

Keywords: Palm Shell Kernel, Activated Carbon, Ethylenediaminetetraacetic Acid, Methylene Blue, Rhodamine B, Real Effluent

1. Introduction

Dyes may impact the aquatic environment quality and human health [1, 2]. Dyes ingestion by Humans cause skin cancer, mental instability, and elevated blood pressure [3]. Dyes contamination can also decrease the ability of the blood to carry vital oxygen throughout the body [4]. However, dyes removal from wastewater are very important. The adsorption technique is commonly used due to remove dye throught

sevarial adsorbents [5-10]. But, these investigations did not focus on improving the activated carbon surface functional groups which can increase the adsorption capacities.

The modification of the surfaces of the adsorbents consists in introducing functional groups such as oxygen and nitrogen on their surfaces. This method generally uses activating and modifying agents. These activating and modifying agents include orthophosphoric acid (H_3PO_4) and ethylenediaminetetraacetic acid (EDTA), respectively.

Orthophosphoric acid is increasingly used in the chemical activation of activated carbons due to its easy recovery and low environmental impact. EDTA is commonly used due to its excellent complexing properties. Several authors used ex-situ modification to improve adsorbents' adsorption properties. Thus, ex-situ EDTA modification of the surface of adsorbents such as bentonite [11], sawdust [12], and graphene oxide [13] improved their adsorption capacities towards methylene blue, brilliant green, and crystal violet, respectively. However, this method is a long and laborious procedure. Thus, in situ modification has been considered. In situ EDTA modification can promote the generation of oxygen functional groups via EDTA carboxyl groups and nitrogen functional groups via EDTA amine groups [14-16]. Therefore, this method can enhance pollutants removal capacities. Li et al. [16] reported that nickel (Ni) removal capacity was enhanced by *Typha orientali*s activated carbon modified in situ by EDTA. Recently, Lv et al. [15] reported that EDTA@bamboo-activated carbon has improved lead (Pb) and copper (Cu) ions adsorption capacities. However, few data are available on the removal of rhodamine B (RhB) and methylene blue (MB) by palm kernel shell modified in situ by EDTA.

The aims of this study were to: (i) synthesize and characterize palm kernel shell activated carbon that had been in situ modified by EDTA, and (ii) explore the feasibility for removing MB and RhB from aqueous solutions and industrial effluent.

2. Materials and Methods

2.1. Materials and Reagents

The reagents such as phosphoric acid H_3PO_4, sodium hydroxide NaOH, chloride acid HCl, methylene blue $C_{16}H_{18}ClN_3S$ and rhodamine B $C_{28}H_{31}ClN_2O_3$ were used. Methylene blue (MB) and rhodamine B (RhB) concentrations were determined using the spectrometer HACH DR 6000 at 664 nm and at 554 nm, respectively.

2.2. Synthesis of the Activated Carbons

Firstly, the palm kernel shells were carbonized at 400 °C for 2 h, in an electric furnace (Advantech KL-280) and were sieved to the particle size of 100 μm [17]. The carbonized shells was mixed with concentration of EDTA 0.1 M and impregnated with H_3PO_4 at an impregnation ratio of 1/1 (g H_3PO_4/g carbonized shells) for 24 h. After heating at 600 °C for 2h in a furnace, the resulting products were cleaned with Milli Q water, and were dried at 80°C in an oven for 24 hours. Finally, the activated carbon without EDTA modification was denoted as AC. Wheras, that with EDTA modification was marked AC-EDTA.

2.3. Characterization of the Activated Carbons: Specific Surface Area, pH at the Point of Zero Charge (pHpzc), and FTIR Analysis

AC and AC-EDTA specific surface areas (S_L) were carried out following the method based on the adsorption of acetic acid [18], and were calculated using the following expression: as follows

$$S_L(m^2/g) = Q_m \times \omega \times \mathcal{N}_A \qquad (1)$$

Q_m (mg/g), ω, and $\mathcal{N}_A$ (mol^{-1}) are the maximum acetic acid adsorption capacity, surface of acetic acid, and Avogadro's number, respectively [17].

The FTIR spectra of the samples were registered using the spectrophotometer Perkin Elmer 100. Activated carbon's pHpzc was determined by setting chloride sodium NaCl concentration at 0.01 mol. L^{-1}, and varying the solution pH from 2 to 12 [17].

2.4. Adsorption Experiments

In the aqueous solution, the adsorption experiments were done at room temperature by varying the contact time (5 - 180 min), the initial dye's concentrations (10 – 50 mg/L), the activated carbon mass (0.025 – 0.3 g), and the pH (2 - 11). The pH was adjusted using either HCl (0.5 mol. L^{-1}) or NaOH (0.5 mol. L^{-1}).

A mass of 0.2 g of AC or AC-EDTA was added to 20 mL of the realwastewater collected around a paint processing plant in Abidjan City (Côte d'Ivoire), and the suspensions were continuously stirred for two hours [17].

The adsorption percentage, and the dye adsorption capacities were computed using the equations (2), (3), and (4), respectively:

$$\% \text{ Ads } = \frac{(C_0 - C_e) \times 100}{C_0} \qquad (2)$$

$$q_t = \frac{(C_0 - C_t) \times V}{m} \qquad (3)$$

$$q_e = \frac{(C_0 - C_e) \times V}{m} \qquad (4)$$

C_0 (mg/L): dye's initial concentration

C_e (mg/L): dye's concentration at equilibrium are the initial and equilibrium concentrations of MB or RhB,

C_t (mg/L): dye's concentration at time t

V (mL), and m (g) are the solution's volume, and the activated carbon's mass, respectively.

3. Results and Discussion

3.1. Physicochemical Characteristics of the Activated Carbons

3.1.1. pH$_{PZC}$, and Specific Surface Area (S_L)

In the Figure 1, the results indicated pH$_{PZC}$ values of 5.4 and 4.1 for AC and AC-EDTA, respectively, indicating their acidic character. The S_L values were 756 m^2/g and 538 m^2/g for AC and AC-EDTA, respectively. The specific surface areas decreased with the modified activated carbon (AC-EDTA). That can be explained by the blockage of the micropores by the EDTA during the impregnation process [19]. In addition, the values of the specific surfaces showed that phosphoric acid is efficient in developing pores in

activated carbons.

3.1.2. FTIR and Raman Spectra Analysis

The FTIR results of AC and AC-EDTA are given in Figure 2. The FTIR of AC showed different peaks at 3377 cm^{-1}, 2965 cm^{-1}, 1561 cm^{-1} and 1040 cm^{-1}. According to Kumar and Jena [20], the band at 3377 cm^{-1} is attributed to O–H stretching of hydroxyl groups from carboxyls, phenols, or alcohols and adsorbed water. While at 1040 cm^{-1} the peak is assigned to C-O stretching in acids, alcohols, phenols, ethers, and esters [20]. The signal obtained at 2970 cm^{-1} is assigned to an aliphatic–CH stretching [21]. The band at 1561 cm^{-1} indicates the presence of the C=C stretching vibration [21, 22]. The FITR of AC indicates the presence of stretching vibration of -

O-C in P-O-C of aromatic and stretching vibration of P=OOH at 1040 cm^{-1} [23]. With modified activated carbon (AC-EDTA), the band at 3658 cm^{-1} is attributed to O–H stretching. The signal observed at 2970 cm^{-1} can be assigned to an aliphatic–CH stretching of the methyl group. This band is broader than that observed with AC due to the presence of EDTA. The peak at 1682 cm^{-1} can be attributed to C=O stretching vibration in –NHCO. According to Keyvani et al. [22], the peak observed at 1040 cm^{-1} indicates the C-N bond of EDTA. In addition, the AC-EDTA presents a peak for N-H at 1561 cm^{-1}. The peaks of C-N, N-H, and C=O functional groups were not present in the AC spectra. Therefore, EDTA has been successfully attached to the surface of AC.
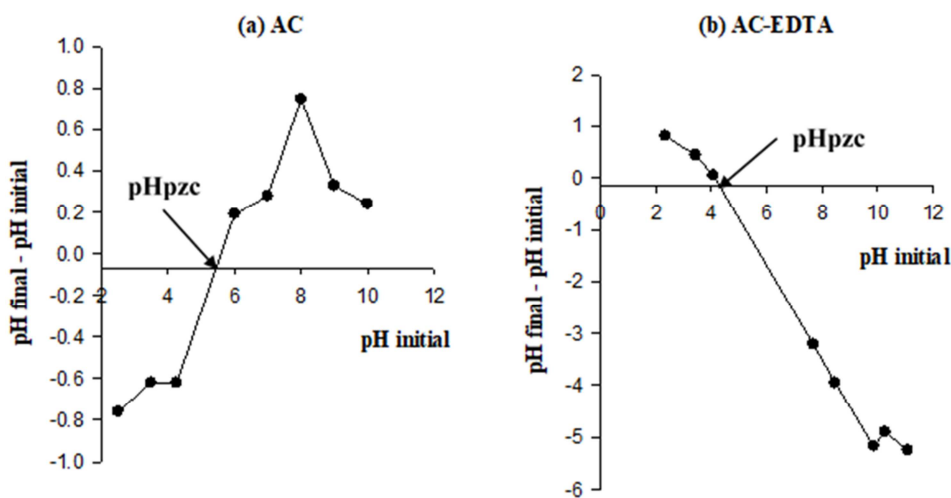

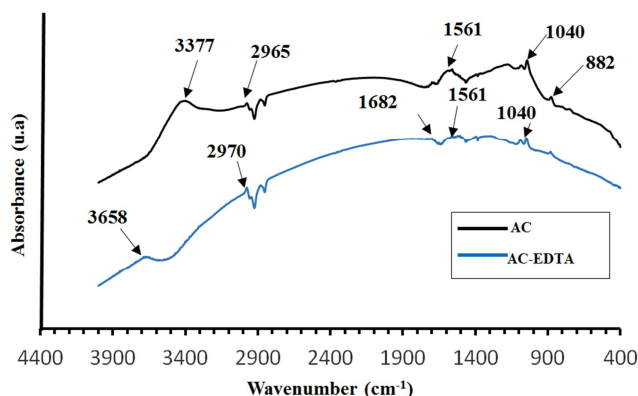**Figure 1.** *pH at the Point of Zero Charge (pH$_{pzc}$).*

Figure 2. *FTIR Spectra of AC and AC-EDTA.*

According to Figure 3, both for AC and AC-EDTA, two wides trips were observed close 1300 cm^{-1} and 1500 cm^{-1}. At 1592 cm^{-1} (for AC-EDTA) and 1596 cm^{-1} (for AC), the peaks (G peak) reveal the presence of graphite [24]. While, the bands (D band) at 1357 cm^{1} (foer AC-EDTA) and 1344 cm^{-1} (for AC) are attributed to a disorder in the carbon structure [24]. The evaluation of the degree of graphitization via the following relationship $R = \frac{I_D}{I_G}$ [24], gave R values of 0.63 and 0.78 for AC and AC-EDTA, respectively. The highest R value obtained with AC-EDTA (0.78) could be explained by the

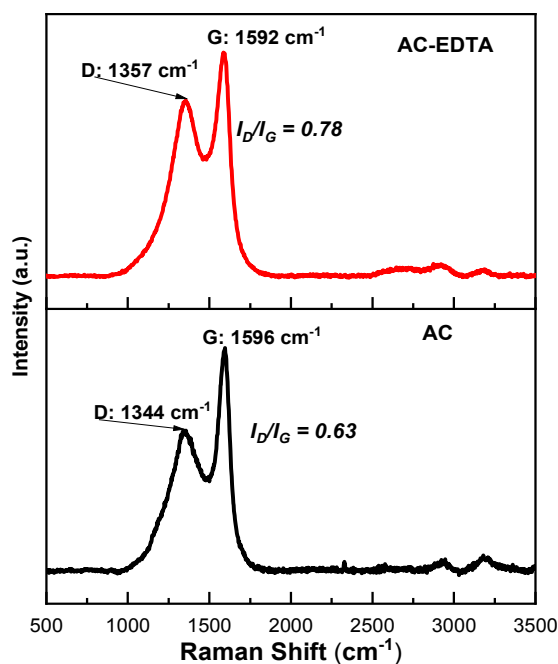modification of AC by EDTA. These results are consistent with those of the FITR analysis.

Figure 3. *Raman spectra of Unmodified Activated Carbon (AC) and Modified Activated Carbon (AC-EDTA).*

3.2. MB, and RhB Adsorption over the Time

Dyes' adsorption capacities increased rapidly during the initial adsorption stages and slowly near equilibrium (Figure 4) due to the availability of adsorption sites [25]. The occupation of these sites during the adsorption process decreases the diffusion of MB and RhB [26]. MB maximum adsorption capacities were 4.19 mg/g (at 45 min) and 7.20 mg/g (at 120 min) for AC and AC-EDTA, respectively. Those for RhB were 2.80 mg/g (at 90 min) and 4.79 mg/g (at 45 min) for AC and AC-EDTA, respectively.
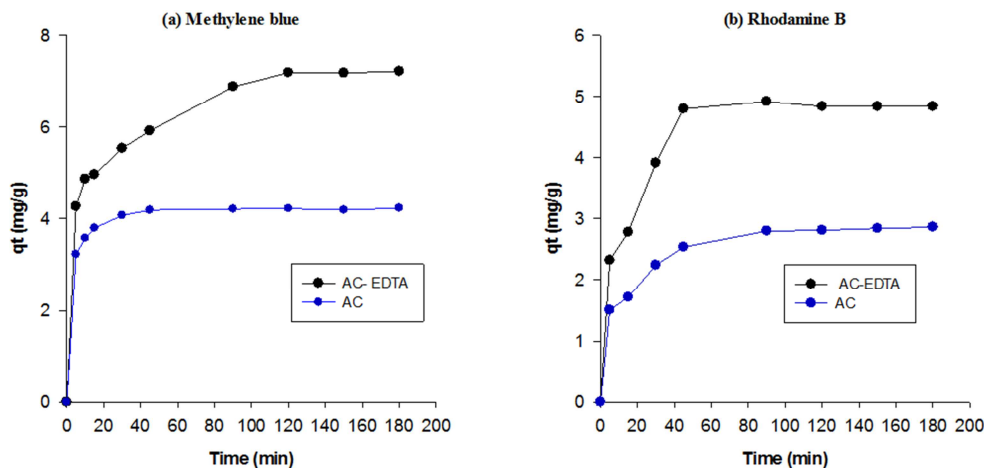

Figure 4. *Effect of Contact Time on Adsorption Capacities of Methylene Blue (a) and Rhodamine B (b) by Activated Carbons.*

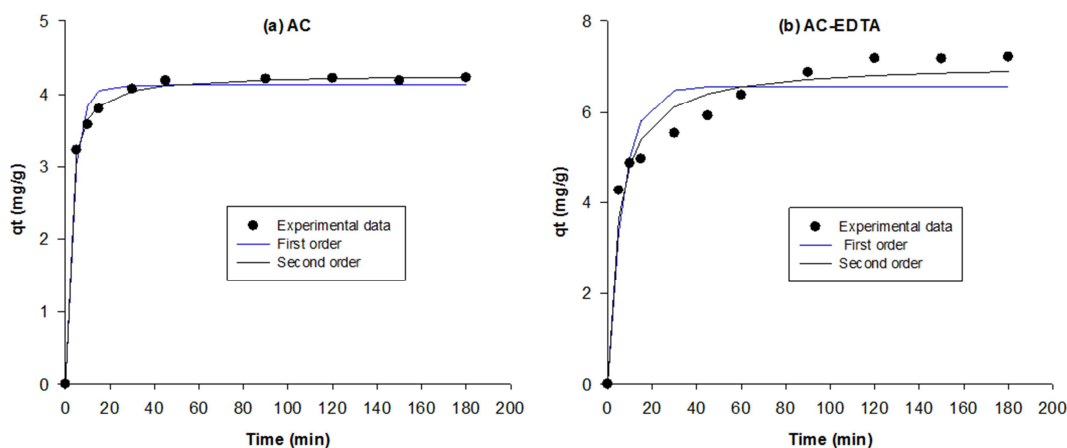The kinetic data were fitted by nonlinear regression analysis (Figures 5 and 6).

Figure 5. *Adsorption Kinetics: Nonlinear Pseudo-First Order Model and Nonlinear Pseudo-Second-Order Model for Removal of Methylene Blue.*
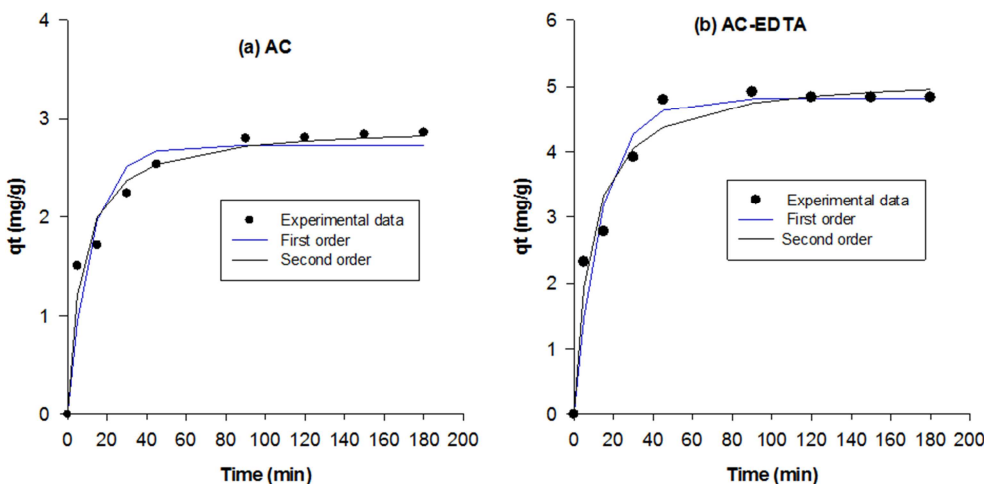

Figure 6. *Adsorption Kinetics: Nonlinear Pseudo-First Order Model and Nonlinear Pseudo-Second-Order Model for Removal of Rhodamine B.*

The nonlinear forms of the pseudo-first-order model [27], and the pseudo-second-order model [28], were given by equation (5) and equation (6), respectively:

$$q_t = q_e[1 - \exp(-k_1 t)] \qquad (5)$$

$$q_t = \frac{q_e^2 k_2 t}{1 + q_e k_2 t} \qquad (6)$$

In eqs. (6) and (7), k_1, and k_2 are the pseudo-first-order, and the pseudo second-order rate constants, respectively.

An error analysis based on the Sum of Squares Errors (SSE), and the Chi-square (χ^2) were performed in this study. The following equations (7) and (8) give the expression of the SSE and χ^2.

$$SSE = \sum_{i=1}^{n}(q_{e\,exp} - q_{e\,cal})^2 \qquad (7)$$

$$\chi^2 = \sum_{i=1}^{n} \frac{(q_{e\,exp} - q_{e\,cal})^2}{q_{e\,cal}} \qquad (8)$$

qe exp and qecal are experimental and predicted adsorption capacities, respectively.

The pseudo-second-order controls MB and RhB adsorption, indicated by the lowest values of (χ^2) and SSE obtained through pseudo-second-order (Table 1). Both for AC and AC-EDTA, the carboxylic and amino groups of the activated carbons electrostatically attract the dyes, thereby resulting in chemisorption [28]. Several authors such as Kataria and Garg [28], Ramutshatsha-Makhwedzha et al. [29], Ahmad et al. [30], and Han et al. [31] have also observed that chemical processes govern methylene blue dye adsorption using sawdust, orange peels, peanut shells, and eucalyptus, respectively.

Table 1. Parameters of Pseudo-First-Order, Pseudo-Second-Order, Langmuir, Freundlich, and Sips Models Using Non Linear Analysis.

			Methylene blue (MB)		Rhodamine B (RhB)	
	Qexp (mg/g)	**AC** MB: 4.19 / RhB: 2.80				
		AC-EDTA MB: 7.20 / RhB: 4.79	**AC**	**AC-EDTA**	**AC**	**AC-EDTA**
Kinetic	Pseudo first order	Qe_1 (mg/g)	4.125	6.577	2.734	4.816
		k_1	0.265	0.142	0.085	0.072
		χ^2	0.052	0.760	0.419	0.593
		SSE	0.196	4.150	0.531	1.071
		R^2	0.9931	0.9516	0.918	0.946
	Pseudo second order	Qe_2 (mg/g)	4.277	7.080	2.937	5.186
		k_2	0.135	0.030	0.048	0.023
		χ^2	0.004	0.290	0.121	0.222
		SSE	0.016	1.54	0.191	0.697
		R^2	0.9995	0.9822	0.969	0.965
Isotherm	Langmiur	$Qmax$ (mg/g)	5.50	7.40	3.82	7.11
		K_L	0.2979	1.370	0.0350	0.0617
		R_L	0.063	0.019	0.571	0.324
		χ^2	0.034	0.076	0.023	0.007
		SSE	0.106	0.415	0.031	0.011
		R^2	0.9973	0.9984	0.9903	0.9992
	Freudlich	K_F	1.799	3.726	0.2445	0.7774
		n	2.987	3.677	1.6414	1.885
		χ^2	0.067	0.434	0.064	0.052
		SSE	0.213	1.824	0.083	0.134
		R^2	0.9946	0.9773	0.9745	0.9904
	Sips	K_S	0.2773	1.3445	0.021	0.0631
		m_s	0.7201	0.9825	1.4248	0.9450
		χ^2	0.006	0.0260	0.009	0.005
		SSE	0.0228	0.1094	0.142	0.009
		R^2	0.9982	0.9957	0.9945	0.9992

3.3. Adsorption Capacities of MB, and RhB in Aqueous Solutions

When the dye's initial concentration is raised from 10 mg/L to 50 mg/L, the dye's removal percentages for both adsorbents decreased (Figure 7), with an optimum percentage at 10 mg/L.

The activated carbons AC and AC-EDTA had good adsorption capacities toward MB and Rh B (Figure 8). The nonlinear analysis was used to fit the isotherm adsorption data (Table 1, Figures 9 and 10). The non linear forms of Langmuir [32], Freundlich [33], and Sips [34] adsorption models were given by Eqs. (9), (10), and (11), respectively:

$$Q_e = \frac{Q_{max} \times K_L \times C_e}{1 + (K_L \times C_e)} \qquad (9)$$

$$Q_e = K_F \times C_e^{1/n} \qquad (10)$$

$$Q_e = \frac{Q_{ms} \times K_S \times C_e^{ms}}{1 + K_S \times C_e^{ms}} \qquad (11)$$

C_e (mg/L) is the equilibrium dye concentration; Qe (mg/g) represents the adsorption capacity of dye, K_L (L/mg), K_F, and K_S are the Langmuir, Freundlich, and Sips constants, respectively. Q_{max} (mg/g) and Q_{ms} (mg/g) are the Langmuir and Sips maximum adsorption capacities, respectively. *n* and *m* are the Freundlich, and Sips models exponents, respectively [3]. For each dye, the Langmuir χ^2 and SSE, for both AC and

AC-EDTA were lower than those of the Freundlich model. In addition, the Langmuir SSE, K_L, and R^2 values were close to those of Sips. Therefore, the best model to fit MB and RhB adsorption data was the Langmuir model showing a monolayer adsorption process [16]. The results also showed that the values of *n* were above 1 (Table 1), indicating that MB and RhB adsorption on AC and AC-EDTA was favorable. Modified activated carbon (AC-EDTA) has higher MB and RhB adsorption capacities than unmodified activated carbon (AC). Indeed, the K_F values (3.726 with MB and 0.7774 with Rh B) for AC-EDTA were higher than those for AC (1.779 with MB and 0.2445 with RhB). This study also showed that the maximum methylene blue adsorption capacities (Qm)

were 5.50 mg/g, and 7.4 mg/g for AC and AC-EDTA, respectively. Those of rhodamine B were 3.82 mg/g, and 7.11 mg/g for AC and AC-EDTA, respectively. Therefore, methylene blue and rhodamine B adsorption was enhanced with AC-EDTA, due to the formation of new active sites for MB and RhB adsorption. Our findings corroborate those of Liu et al. [14], and Lv et al. [15], who showed that the removal of cationic pollutants was enhanced by in situ EDTA-modified activated carbons. According to Liu et al. [14], Ni adsorption was enhanced by EDTA-*typha orientalis* activated carbon. Lv et al. [15] reported that the removal of Pb and Cu was enhanced by EDTA-bamboo activated carbon.
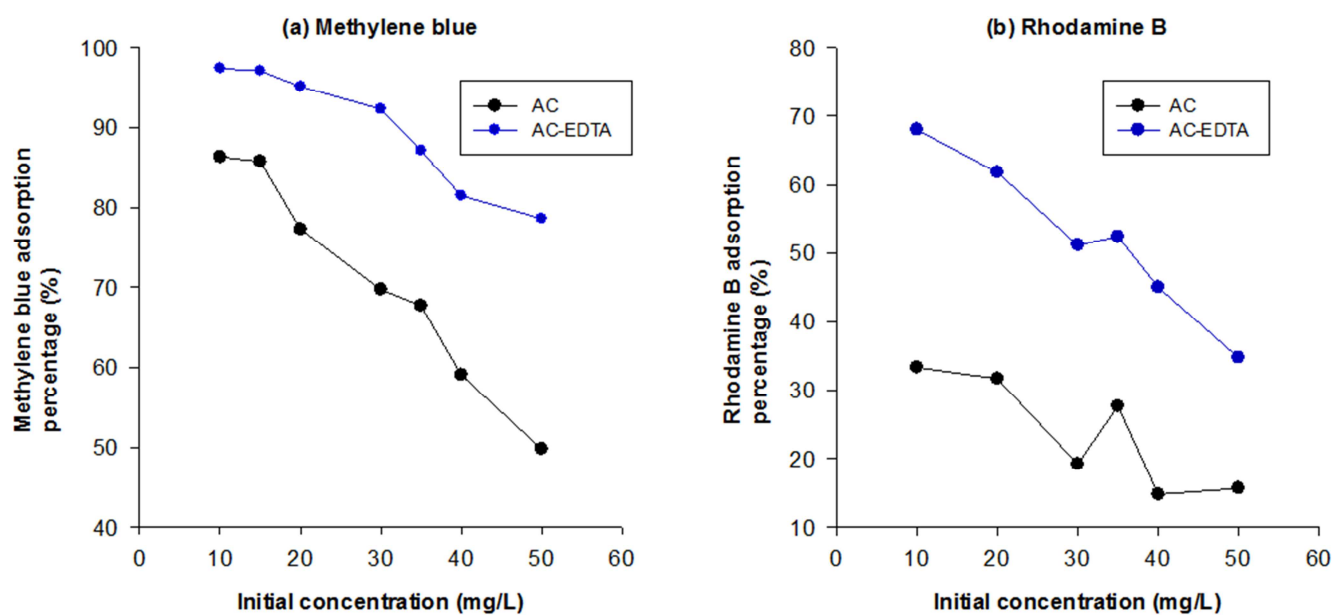

Figure 7. *Effect of Initial Concentration on Methylene Blue (a) and Rhodamine B (b) Removal.*
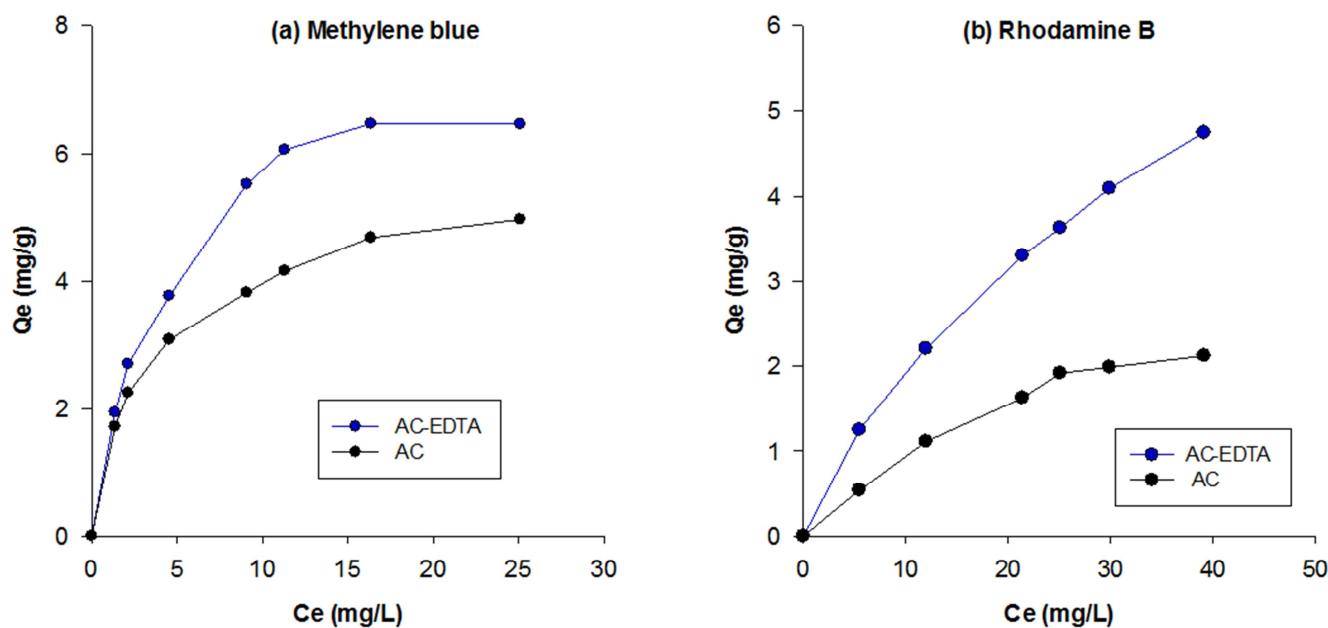

Figure 8. *Adsorption Isotherms of Methylene Blue (a) and Rhodamine B (b).*
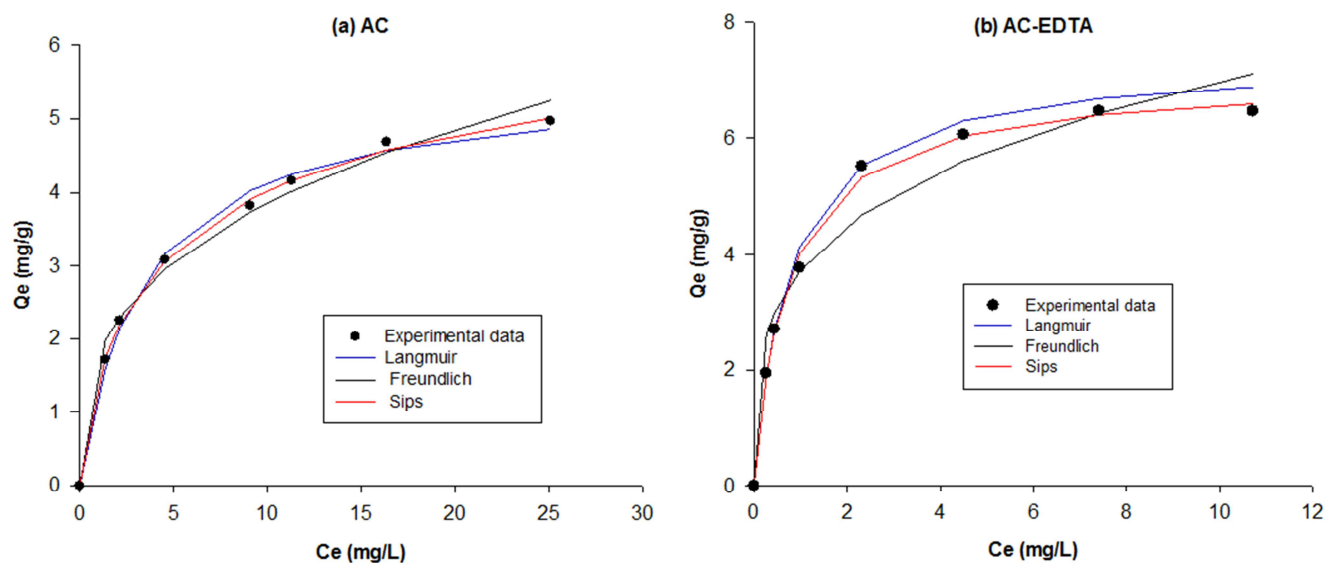
Figure 9. Nonlinear Langmuir Isotherm, Nonlinear Freundlich Isotherm, and Nonlinear Sips Isotherm for Methylene Blue Adsorptio.
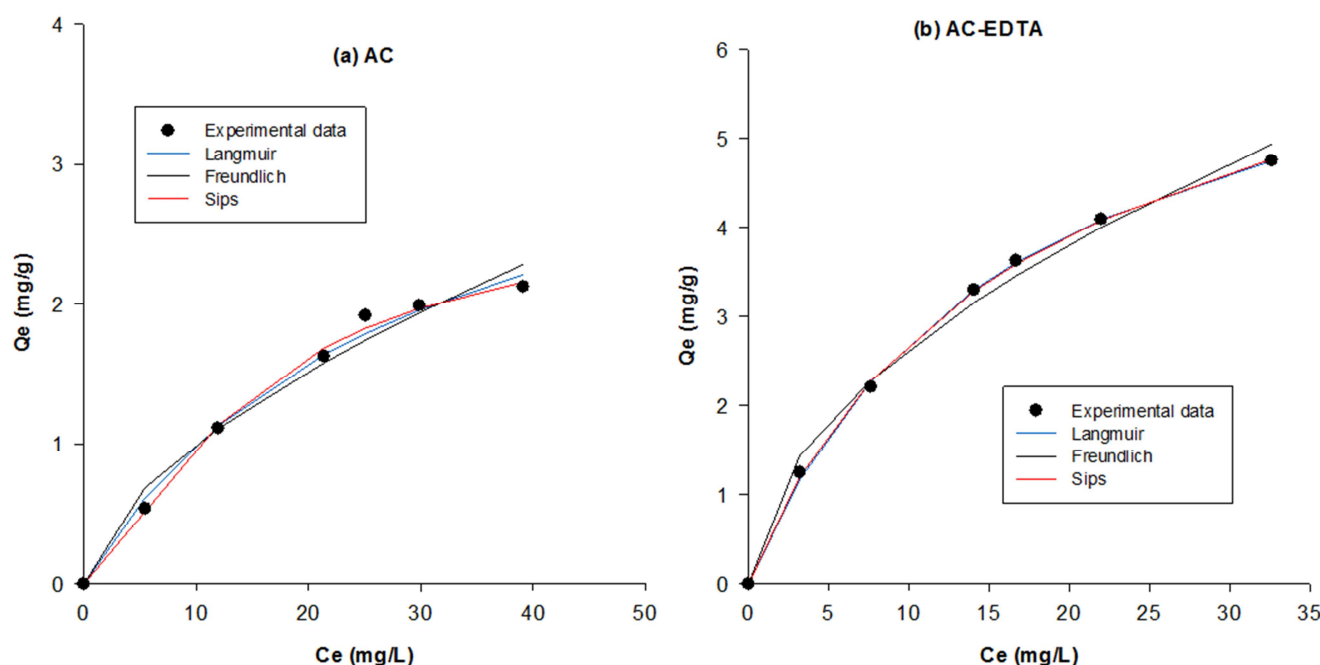

Figure 10. Nonlinear Langmuir Isotherm, Nonlinear Freundlich Isotherm, and Nonlinear Sips Isotherm for Rhodamine B Adsorptio.

The methylene blue and rhodamine B maximum adsorption capacities (Q_m) obtained in the present investigation were contrasted with those from the literature (Table 2). The results showed that data for methylene blue from the present study were comparable to those reported by Kavitha and Namasivayan [35], Cengiz and Cavas [36], Pekkuz et al. [37],

and Sharma and Uma [38]. Rhodamine B's maximum adsorption capacity (Q_m) from the present study was lower than those reported by Vigneshwaran et al. [39], and Hou et al. [40]. While, those reported by Oyekanmi et al. [41], Thakur and Kaur [42], and Mousavi et al. [43].

Table 2. Comparison of Adsorption Capacities of Different Adsorbents for the Removal of MB and RhB.

Dyes	Adsorbent	Q_m (mg/g)	References
MB	Palm kernel shell unmodified (AC)	5.50	This study
	Palm kernel shell modified (AC-EDTA)	7.40	This study
	Coir pith carbon	5.87	Kavitha and Namasivayam [35]
	Marine seaweed	5.23	Cengiz and Cavas [36]
	Sawdust	4.89	Pekkuz and al. [37]
	Rice husk	9.83	Sharma and Uma [38]

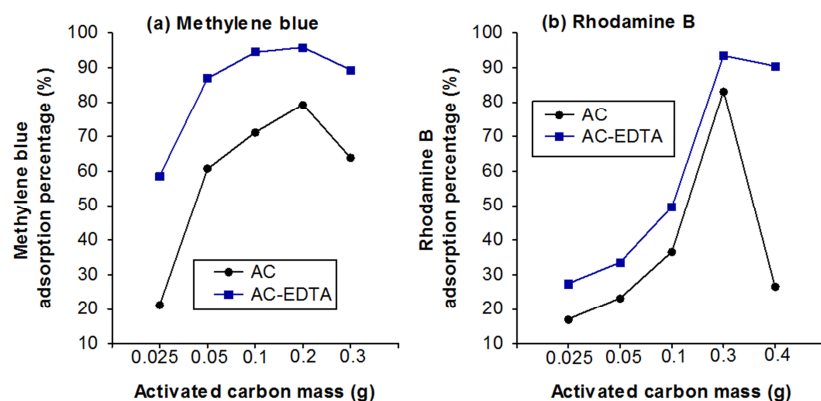| Dyes	Adsorbent	Q_m (mg/g)	References
RhB	Palm kernel shell unmodified (AC)	3.82	This study
	Palm kernel shell modified (AC-EDTA)	7.11	This study
	Topica peel	32.81	Vigneshwaran et al. [39]
	Bamboo shoot shell	25.00	Hou et al.[40]
	Banana peel	9.5	Oyekanmi et al. [41]
	Paper industry waste	6.71	Thakur and Kaur [42]
	Stalk corn	5.3	Mousavi et al. [43]

Figure 11. *Removal Efficiencies of Methylene Blue (a) and Rhodamine B (b) with Different Adsorbent Mass.*
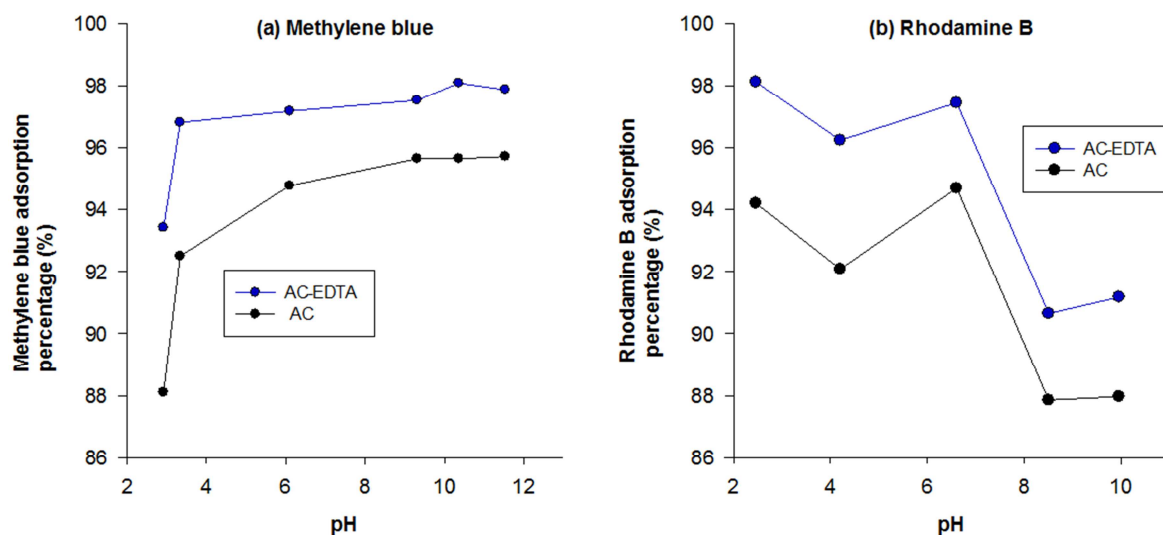

Figure 12. *Effect pH on Adsorption Capacities of Methylene Blue and Rhodamine B.*

3.4. Effect of Adsorbents Mass on MB and RhB Adsorption in Aqueous Solution

Figures 11a and 11b show the effect of AC and AC-EDTA mass on MB and RhB removal. The maximum percentages of methylene blue were 79.35% and 95.87% for AC and AC-EDTA, respectively with an adsorbents mass of 0.2 g. Those of rhodamine B were 83.29% and 93.47% for AC and AC-EDTA, respectively with an adsorbents mass of 0.3 g. Beyond these values, the adsorption rate decreases, which may be caused by the agglomeration of activated carbons [44].

3.5. Adsorption of Dyes Versus Aqueous Solution pH

The effect of pH on methylene blue adsorption is given by Figure 12a. The optimum values of pH were 9.31 for AC (95.64%) and 10.36 for AC-EDTA (98.08%). These optimum values were higher than pHpzc values (5.6 for AC and 4.1 for AC-EDTA). At these pH, the electrostatic attraction phenomena between AC or AC-EDTA and MB $((C_{16}H_{18}N_3Cl^-)S^+)$ can promote methylene blue adsorption [17]. Several authors reported similar observations for methylene blue [28; 29; 45-47] at higher pH. At pH values below 5.6 and 4.1, the percentages of methylene blue adsorption were low, due to electrostatic repulsion phenomenon [17].

The influence of pH on the adsorption of RhB is given in Figure 12b. The adsorption rates of RhB decreased from 94.2% to 87.0% with AC, and from 98.1% to 90.6% with AC-EDTA when the pH is raised from 2 to 10 (Figure 9b).

The maximum adsorption percentages (94.2% for AC, and 98.1% for AC-EDTA) were obtained at pH 2.4. The pH optimum value (pH 2.4) was lower than the pHpzc of AC (5.6) and AC-EDTA (4.1). Below these values of pHpzc, the attraction process among AC or AC-EDTA surface and rhodamine B explained the high adsorption percentages [48, 49]. While, at pH > pHpzc (5.6 or 4.1), the adsorption rates decrease due to the repulsion between AC and AC-EDTA surface negative charge [49]. The higher adsorption capacities of rhodamine B at pH 2.4 may be explained by the fact that rhodamine B exists mainly in the cationic form at pH < 3 and in zwitterion form at pH > 5 (Wu et al. 2020; Xue et al. 2021). At pH < 3, the COOH group on the surface of AC or AC-EDTA reacts with a proton to form $COOH_2^+$, and RhB exists in its positive form (RhB^+) [50]. When the solution's pH increases, the content of the RhB^+ species may decrease due to the predominance of zwiter ion (RhB^+). In addition, the increase in pH of the solution leads to the ionization of the carbonyl group of AC or AC-EDTA to form COO^-, then the hydrogen bond and ion exchange between AC or AC-EDTA and RhB is slightly weakened [50]. Therefore, the rhodamine B adsorption capacities are reduced.

3.6. Removal of MB and RhB from Industrial Effluent

In the real effluent, the adsorption percentages of MB and RhB by AC were 59.83%, and 12.9%, respectively. While, those with AC-EDTA were 79.98 and 58.71% for MB, and RhB, respectively (Table 3). Compared to synthetic solutions, the percentages of dyes adsorbed in industrial effluents were reduced. Indeed, in the synthetic solution, the methylene blue removals percentages by AC and AC-EDTA were 79.35% and 95.87%, respectively. Those of rhodamine B were 83.29% and 93.47%, respectively for AC and AC-EDTA. The decrease in dyes adsorption percentages from the real effluent can be explained by the presence of other chemicals. Considering this study, it appears that the removal percentages with AC-EDTA were higher than those with AC. Thus, the AC-EDTA enhanced MB and RhB removal from industrial effluent.

Table 3. *Industrial Effluent Treatment.*

	Before adsorption (mg/L)	AC			AC-EDTA	
		After adsorption (mg/L)	Adorption percentage (%)		After adsorption (mg/L)	Adsorption percentage (%)
MB	10.72	4.3	59.83		2.14	79.98
RhB	10.83	9.44	12.90		4.47	58.71

4. Conclusion

This study aimed to remove rhodamine B (RhB) and methylene blue (MB) from industrial effluent by palm kernel shell modified activated carbon. The pHpzc values were 5.4 and 4.1 for AC, and AC-EDTA, respectively, indicating their acidic properties. The specific surface areas were found to be 756 m²/g and 538 m²/g for AC and AC-EDTA, respectively. The FTIR results indicated that C-N, N-H, and C=O functional groups were introduced onto the surface of activated carbon after in situ EDTA modification. In synthetic aqueous solutions, the methylene blue adsorption percentages were 95.64% at pH 9.31 for AC and 98.08% at pH 10.36 for AC-EDTA. Whereas, those of rhodamine B were 94.2% for AC, and 98.1% for AC-EDTA at pH 2.4. The results showed that the pseudo-second-order and Langmuir models control MB and RhB adsorption, indicating a chemisorption and monolayer adsorption processes. In addition, methylene blue maximum adsorption capacities (Qmax) were 5.5 mg/g, and 7.40 mg/g for AC, and AC-EDTA, respectively. Rhodamine B's maximum adsorption capacities were 3.82 mg/g, and 7.11 mg/g for AC, and AC-EDTA, respectively. In the real wastewater, methylene blue removals percentages by AC and AC-EDTA were 59.83% and 79.98%, respectively. Those of rhodamine B were 12.9% and 58.71%, respectively for AC and AC-EDTA. Therefore, MB and RhB adsorption were enhanced with AC-EDTA in aqueous solutions, and industrial effluent.

Authors' Contributions

N'guessan Louis Berenger Kouassi, Abollé Abollé, Adjoumani Rodrigue Kouakou, Victor Gogbé, and Albert Trokourey have actively participated in the conceptualization and writing the publication.

Conflict of Interests

All the authors do not have any possible conflicts of interest.

Acknowledgements

References

[1] Cheng J, Zhan C, Wu J, Cui Z, Si J, Wang Q, Peng X, Turng LS (2020) Highly Efficient Removal of Methylene Blue Dye from an Aqueous Solution Using Cellulose Acetate Nanofibrous Membranes Modified by Polydopamine. ACS Omega 5: 5389−5400. https://dx.doi.org/10.1021/acsomega.9b04425

[2] Mehra S, Singh M, Chadha P (2021) Adverse Impact of Textile Dyes on the Aquaticn Environment as well as on Human Beings. Toxicol Int 28 (2): 165-176, https://dx.doi.org/10.18311/ti/2021/v28i2/26798

[3] Kouassi NLB, Doubi BIHG, Diabate D, Blonde LD, Albert T, (2023) Recycling of Alum Sludge for Rhodamine B Removal from Industrial Effluents, Chemistry Africa 6: 485-498, https://dx.doi.org/10.1007/s42250-022-00473-7

[4] Al-Ghouti AA, Sweleh AO (2019) Optimizing textile dye removal by activated carbon prepared from olive stones. Environ Technol Innov 16: 100488. https://doi.org/10.1016/j.eti.2019.100488

[5] Arabpour A, Dan S, Hashemipour H (2021) Preparation and optimization of novel graphene oxide and adsorption isotherm study of methylene blue. Arab J Chem 14: 103003. https://doi.org/10.1016/j.arabjc.2021.103003

[6] Gokce Y, Yaglikci S, Yagmur E, Banford A, Aktas Z (2021) Adsorption behaviour of high performance activated carbon from demineralised low rank coal (Rawdon) for methylene blue and phenol. J Environ Chem Eng 9 (2): 104819. https://doi.org/10.1016/j.jece.2020.104819

[7] Nemr AE, Shoaib AGM, Sikaily AE, Mohamed AEDA, Hassan AF (2021) Evaluation of Cationic Methylene Blue Dye Removal by High Surface Area Mesoporous Activated Carbon Derived from Ulva lactuca. Environ Process 8: 311-332. https://doi.org/10.1007/s40710-020-00487-8

[8] Yu M, Dong H, Zheng Y, Liu W (2021) Ternary metal oxide embedded carbon derived from metal organic frameworks for adsorption of methylene blue and acid red 73. Chemosphere 280: 130567. https://doi.org/10.1016/j.chemosphere.2021.130567

[9] Vedula SS, Yadav GD (2022) Wastewater treatment containing methylene blue dye as pollutant using adsorption by chitosan lignin membrane: Development of membrane, characterization and kinetics of adsorption. J Indian Chem Soc 99: 100263. https://doi.org/10.1016/j.jics.2021.100263

[10] Yadav A, Dindorkar SS, Ramisetti SB, Sinha N (2022) Simultaneous adsorption of methylene blue and arsenic on graphene, boron nitride and boron carbon nitride nanosheets: Insights from molecular simulations. J Water Process Eng 46: 102653. https://doi.org/10.1016/j.jwpe.2022.102653

[11] Maria LFADC, Abad MMLB, Divine Angela G. Sumalinog DAG, Abarca RRM, Peerasak Paoprasert P, Luna MDGD (2018) Adsorption of Methylene Blue dye and Cu(II) ions on EDTA-modified bentonite: Isotherm, kinetic and thermodynamic studies. Sustain Environ Res 28: 197-205. https://doi.org/10.1016/j.serj.2018.04.001

[12] Kataria N, Garg VK (2019) Application of EDTA modified Fe_3O_4/sawdust carbon nanocomposites to ameliorate methylene blue and brilliant green dye laden water. Environ Res 172: 43–54. https://doi.org/10.1016/j.envres.2019.02.002

[13] Wang H, Lai X, Zhao W, Chen Y, Yang X, Meng X, Li Y (2019) Efficient removal of crystal violet dye using EDTA/ graphene oxide functionalized corncob: A novel low cost adsorbent. RSC Advances 9: 21996. https://doi.org/10.1039/c9ra04003j

[14] Jeskey J, Chen Y, Kim S, Xia Y (2023) EDTA-Assisted Synthesis of Nitrogen-Doped Carbon Nanospheres with Uniform Sizes for Photonic and Electrocatalytic Applications. Chem. Mater 35: 3024−3032. https://doi.org/10.1021/acs.chemmater.3c00341

[15] Lv D, Liu Y, Zhou J, Yang K, Lou Z, Baig SA, Xu X (2018) Application of EDTA-functionalized bamboo activated carbon (BAC) for Pb(II) and Cu(II) removal from aqueous solutions. Appl Surf Sci 428.648-658. https://doi.org/10.1016/j.apsusc.2017.09.151

[16] Li Y, Zhang J, Liu H (2018) In-situ modification of activated carbon with ethylenediaminetetraacetic acid disodium salt during phosphoric acid activation for enhancement of nickel removal. Powder Technol 325: 113–120. https://doi.org/10.1016/j.powtec.2017.10.051

[17] Kouassi NLB, N'goran KPDA, Blonde LD, Diabate D, Trokourey A (2023) Simultaneous Removal of Copper and Lead from Industrial Effluents Using Corn Cob Activated Carbon, Chemistry Africa 6: 733-745 https://doi.org/10.1007/s42250-022-00432-2

[18] Kra DO, Allou, NB, Atheba P, Drogui P, Trokourey A (2019) Preparation and Characterization of Activated Carbon Based on Wood (Acacia auriculeaformis, Côte d'Ivoire). J Encapsulation Adsorpt Sci 9: 63-82. https://doi.org/10.4236/jeas.2019.92004

[19] Ezzeddine Z, Batonneau-Gener I, Pouilloux Y, Hamad H, Saad Z, Kazpard V (2015) Divalent heavy metals adsorption onto different types of EDTA-modified mesoporous materials: Effectiveness and complexation rate. Micropor Mesopor 212: 125-136. https://doi.org/10.1016/j.micromeso.2015.03.013

[20] Kumar A, Jena HM (2016) Preparation and characterization of high surface area activated carbon from Fox nut (Euryale ferox) shell by chemical activation with H_3PO_4. Results in Physics 6: 651–658. https://doi.org/10.1016/j.rinp.2016.09.012.

[21] Andia JM, Larrea A, Salcedo J, Reyes J, Lopez L, Yokoyama L (2020) Synthesis and characterization of chemically activated carbon from Passiflora ligularis, Inga feuilleei and native plants of South America. J Environ Chem Eng 8 (4): 103892. https://doi.org/10.1016/j.jece.2020.103892

[22] Keyvani F, Rahpeima S, Javanbakht V (2018) Synthesis of EDTA-modified magnetic activated carbon nanocomposite for removal of permanganate from aqueous solutions. Solid State Sci 83: 31-42. https://doi.org/10.1016/j.solidstatesciences.2018.06.007

[23] Xu J, Chen L, Qu H, Jiao Y, Xie J, Xing G (2014) Preparation and characterization of activated carbon from reedy grassleaves by chemical activation with H_3PO_4. Appl Surf Sci 320: 674–680. https://doi.org/10.1016/j.apsusc.2014.08.178

[24] Liu Y, Liu X, Dong W, Zhang L, Kong Q, Wang W (2017) Efficient Adsorption of Sulfamethazine onto Modified Activated Carbon: A Plausible Adsorption Mechanism. Sci Rep 7, 12437. https://doi.org/10.1038/s41598-017-12805-6

[25] Ozdes D, Gundogdu A, Duran C, Senturk HB (2010) Evaluation of Adsorption Characteristics of Malachite Green onto Almond Shell (Prunus dulcis), Sep Sci Technol. 45: 2076-2085, https://doi.org/10.1080/01496395.2010.504479

[26] Brito MJP, Veloso CM, Santos LS, Bonomo RCF, Fontan RDCI (2018) Adsorption of the textile dye Dianix® royal blue CC onto carbons obtained from yellow mombin fruit stones and activated with KOH and H_3PO_4: kinetics, adsorption equilibrium and thermodynamic studies. Powder Technol 339: 334-343. https://doi.org/10.1016/j.powtec.2018.08.017

[27] Lagergren S (1898) About the theory of so-called adsorption of soluble substances. Kungliga Svenska Vetensk Handl 24: 1–39.

[28] Ho YS, McKay G (1999) Pseudo-second order model for sorption processes. Process Biochem 34: 451–465. https://doi.org/10.1016/S0032-9592 (98)00112-5

[29] Ramutshatsha-Makhwedzha D, Mavhungu A, Moropeng LM, Mbaya R (2022) Activated carbon derived from waste orange and lemon peels for the adsorption of methyl orange and methylene blue dyes from wastewater. Heliyon. https://doi.org/10.1016/j.heliyon.2022.e09930

[30] Ahmad MA, Yusop MFM, Zakaria R, Jamilah Karim J, Yahaya NKEM, Yusoff MAM, Hashim NHF, Abdullah NS (2021) Adsorption of methylene blue from aqueous solution by peanut shell based activated carbon. Mater Today 47: 1246-1251. https://doi.org/10.1016/j.matpr.2021.02.789

[31] Han Q, Wang J, Goodman BA, Xie J, Liu Z (2020) High adsorption of methylene blue by activated carbon prepared from phosphoric acid treated eucalyptus residue. Powder Technol 366: 239–248. https://doi.org/10.1016/j.powtec.2020.02.013

[32] Langmuir I (1906) The adsorption of gases on plane surfaces of glass mica and platinum. J Am Chem Soc 40: 1361–1403.

[33] Freundlich HMF (1906) Über die adsorption in lösungen. Z. PhysChem-Frankfurt 57A: 385-470.

[34] Saruchi, Kumar V (2019) Adsorption kinetics and isotherms for the removal of rhodamine B dye and $Pb+2$ ions from aqueous solutions by a hybrid ion-exchanger. Arab J Chem 12: 316–329. http://dx.doi.org/10.1016/j.arabjc.2016.11.009

[35] Kavitha D, Namasivayam C (2007) Experimental and kinetic studies on methylene blue adsorption by coir pith carbon. Bioresour Technol 98: 14–21. https://doi.org/10.1016/j.biortech.2005.12.008

[36] Cengiz S, Cavas L (2008) Removal of methylene blue by invasive marine seaweed: Caulerpa racemosa var. cylindracea. Bioresour Technol 99: 2357–2363. https://doi.org/10.1016/j.biortech.2007.05.011

[37] Pekkuz H, Uzun I, Güzel F (2008) Kinetics and thermodynamics of the adsorption of some dyestuffs from aqueous solution by poplar sawdust. Bioresour Technol 99: 2009–2017. https://doi.org/10.1016/j.biortech.2007.03.014

[38] Sharma YC, Uma (2010) Optimization of Parameters for Adsorption of Methylene Blue on a Low-Cost Activated Carbon. J Chem Eng Data 55: 435–439. https://doi.org/10.1021/je900408s

[39] Vigneshwaran S, Sirajudheen P, Karthikeyan P, Meenakshi S (2021) Fabrication of sulfur-doped biochar derived from tapioca peel waste with superior adsorption performance for the removal of Malachite green and Rhodamine B dyes. Surf Interfaces 23: 100920. https://doi.org/10.1016/j.surfin.2020.100920

[40] Hou Y, Huang G, Li J, Yang Q, Huang S, Cai J (2019) Hydrothermal conversion of bamboo shoot shell to biochar: Preliminary studies of adsorption equilibrium and kinetics for rhodamine B removal. J Anal Appl Pyrolysis 143: 104694. https://doi.org/10.1016/j.jaap.2019.104694

[41] Oyekanmi AA, Ahmad A, Hossain K, Rafatullah M (2019) Adsorption of Rhodamine B dye from aqueous solution onto acid treated banana peel: Response surface methodology, kinetics and isotherm studies. PloS One 14: 1-20. https://doi.org/10.1371/journal.pone.0216878

[42] Thakur A, Kaur H (2017) Response surface optimization of Rhodamine B dye removal using paper industry waste as adsorbent. Int J Ind Chem 8: 175–186. http://dx.doi.org/10.1007/s40090-017-0113-4

[43] Mousavi SA, Kamarehie B, Almasi A, Darvishmotevalli M, Salari M, Moradnia M, Azimi F, Ghaderpoori M, Neyazi Z, Karami MA (2021) Removal of Rhodamine B from aqueous solution by stalk corn activated carbon: adsorption and kinetic study. Biomass Convers Biorefin. https://doi.org/10.1007/s13399-021-01628-1

[44] Thomas P, Rumjit NP, Lai CW, Johan MRB (2021) EDTA functionalised cocoa pod carbon encapsulated SPIONs via green synthesis route to ameliorate textile dyes - Kinetics, isotherms, central composite design and artificial neural network. Sustain Chem Pharm 19: 100349. https://doi.org/10.1016/j.scp.2020.100349

[45] Song M, Wei Y, Cai S, Yu L, Zhong Z, Jin B (2018) Study on adsorption properties and mechanism of Pb^{2+} with different carbon based adsorbents. Sci Total Environ 618: 1416-1422. https://doi.org/10.1016/j.scitotenv.2017.09.268

[46] Xia Y, Yao Q, Zhang W, Zhang Y, Maojun Zhao M (2019) Comparative adsorption of methylene blue by magnetic baker's yeast and EDTAD-modified magnetic baker's yeast: Equilibrium and kinetic study. Arab J Chem 12: 2448–2456. http://dx.doi.org/10.1016/j.arabjc.2015.03.010

[47] Benjelloun M, Miyah Y, Bouslamti R, Nahali L, Mejbar F, Lairini S (2022) The Fast-Efcient Adsorption Process of the Toxic Dye onto Shells Powders of Walnut and Peanut: Experiments, Equilibrium, Thermodynamic, and Regeneration Studies. Chemistry Africa 5: 375-393. https://doi.org/10.1007/s42250-022-00328-1

[48] Wu J, Yang J, Huang G, Xu C, Lin B (2020) Hydrothermal carbonization synthesis of cassava slag biochar with excellent adsorption performance for Rhodamine B. J Clean Prod 251: 119717. https://doi.org/10.1016/j.jclepro.2019.119717

[49] Kausar A, Shahzad R, Asim S, BiBi S, Iqbal J, Muhammad N, Sillanpaa M, Din IU (2021) Experimental and theoretical studies of Rhodamine B direct dye sorption onto clay-cellulose composite. J Mol Liq 328: 115165. https://doi.org/10.1016/j.molliq.2020.115165

[50] Xue S, Tu B, Li Z, Ma X, Xu Y, Li M, Fang C, Tao H (2021) Enhanced adsorption of Rhodamine B over Zoysia sinica Hance-based carbon activated by amminium chloride and sodium hydroxide treatments. Colloids Surf A Physicochem Eng 618: 126489. https://doi.org/10.1016/j.colsurfa.2021.126489